Biosilica Electrically-Insulating Layers by Soft Lithography-Assisted Biomineralisation with Recombinant Silicatein

*Alessandro Polini, Stefano Pagliara, Andrea Camposeo, Adriana Biasco, Heinz C. Schröder, Werner E. G. Müller, and Dario Pisignano**

Silica films are widely used in many fields, such as coatings and functionalization layers for biomedical surfaces and tissue engineering, controlled drug delivery, transplants, cell adhesion, growth, and controlled differentiation.[1–6] Other applications include masters and moulds for soft and nanoimprint lithographies,[7] diagnostics, optics and optoelectronics, and micro- and nano-electronics.[8] Silica layers with electrically-insulating properties are especially useful as gate dielectrics for field-effect transistors and sensing devices, which today attract increasing interest in the field of organic electronics.[8]

The conventional production of silica surfaces is carried out by processing at extreme temperatures and pressures, and in strongly acid and basic environments.[9] The production of silica by low-cost, gentle biomineralization processes combined with the controlled realization of silica patterns could be instead a feasible and powerful method for the realization of layers, and ultimately devices, by a physiological approach. In fact, differently from industrial manufacturing, the biological synthesis of silica takes place under mild conditions, at low temperatures and pressures and at near-neutral pH, with clear advantages in terms of cost-effectiveness and environmental impact.[10] For instance, some peculiar proteins, named silicateins, contained in the axial filament of siliceous spicules of sponges, are known to catalyze the reaction of silica polymerization.[11] So far, several isoforms of silicatein have been cloned from both marine and freshwater sponges.[11] With mild pH conditions, the silicatein filaments and their constituent subunits are able to catalyze the *in-vitro* polymerization of silica and silsesquioxanes from tetraethoxysilane and organically-modified silicon triethoxides, respectively. Silicatein catalyzes the *polycondensation* of silica thus mediating enzymatically-controlled biomineralization.[10,12] Besides this catalytic activity, upon assembling into mesoscopic filaments (with diameter in the μm range and length up to a few mm), the protein serves as active scaffold that spatially directs the synthesis of polysiloxanes.[13,14] Hence, these biomolecules present combined characteristics of chemical action (catalysis) and patterning potential, by specifically driving silica formation. Unfortunately, while the optical properties of biomineralized structures have been studied because of the resemblance of sponges spicules with optical fibers,[15] nothing is known about their electrical properties and potentiality as insulator materials.

The most abundant silicatein subunit in marine sponges (silicatein-α) is found to be similar to the protein cathepsin L, that exhibits specific cysteine residues forming intramolecular disulfides. Site-directed mutagenesis experiments show that the specific serine (Ser26) and histidine (His165) residues are crucially involved in the catalysis of silica polymerization by silicon alkoxides.[10] Specific expression conditions[16] may be exploited to obtain highly-active proteins. Recombinant routes to silicateins are especially important since they allow to overcome the time-consuming, laborious and low-throughput isolation from natural sources, which would require sacrificing many living organisms.

Polypeptides and polyamines are used to template silica formation by various methods, e. g. electrostatic deposition, direct writing assembly, holographic patterning, photolithography, and surface-initiated polymerization.[17] Proteins such as lysozyme[18] and bovine serum albumin (BSA) in combination with polyelectrolytes[19] are utilized to produce silica-coated surfaces, exploiting the amount of charge available at the surface. More biomimetic approaches are developed by few groups by specific enzymatic routes. Tahir et al. immobilize recombinant silicatein on nitrilotriacetic acid (NTA) terminated alkanethiol-functionalized Au surfaces.[20] Ray and Perry use recombinant silicatein for achieving uniform silica films on Au-coated surfaces through amine immobilization.[21]

Here, we report a novel approach for realizing layers of silica exploiting the enzymatic activity of immobilized recombinant silicatein, and demonstrate for the first time the properties of biomineralized films as electrical insulators potentially usable in bio- and micro-electronic applications (Patent pending). The selective immobilization of the recombinant protein is carried out by the microcontact printing (μCP) technology,[22] which well balances simplicity, low cost, reproducibility, and high filling efficiency of the treated surface.[23] Silica microstructures or films are obtained by simply varying the biomineralisation time (t_{inc}), making this technique appealing for realizing biomineralized inorganic films on different surfaces.

Aiming to capitalizing on the capability of recombinant silicatein in promoting biosilica formation,[10,16,21] and in retaining

Dr. A. Polini, Dr. S. Pagliara, Dr. A. Camposeo, Dr. A. Biasco, Prof. D. Pisignano
at National Nanotechnology Laboratory of Istituto Nanoscienze-CNR
Università del Salento
via Arnesano, I-73100 Lecce, Italy
E-mail: dario.pisignano@unisalento.it
Prof. D. Pisignano
Dipartimento di Ingegneria dell'Innovazione, Università del Salento, via Arnesano, I-73100 Lecce, Italy
Prof. H. C. Schröder, Prof. W. E. G. Müller
at Institute for Physiological Chemistry
University Medical Center of the Johannes Gutenberg University
Duesbergweg 6, D-55099 Mainz, Germany

DOI: 10.1002/adma.201102691

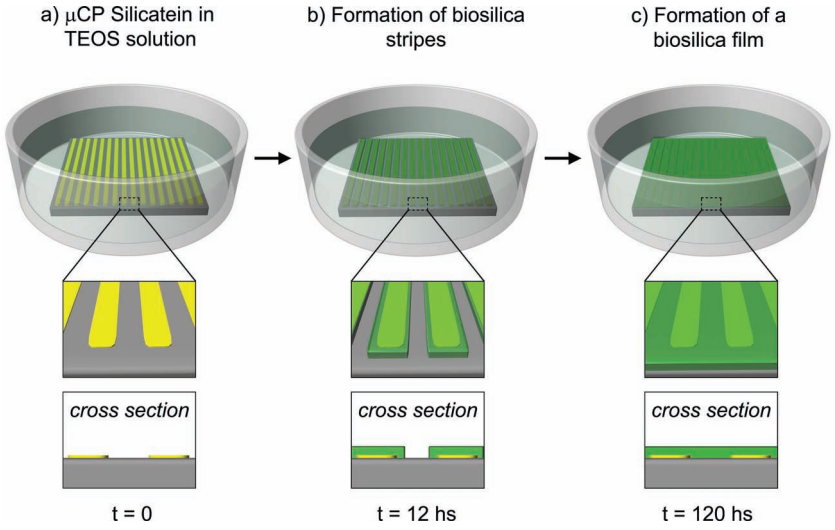

Figure 1. Schematics of production of biosilica layers. Silicatein patterns incubated in silica precursor solution (a). Early formation of biosilica microstructures (b). Formation of silica layers (c). The corresponding cross-sectional schemes for each step are shown in the bottom insets. Yellow features indicate printed silicatein, whereas green regions indicate biosilica mineralized on top of the protein.

its pristine catalyzing and directing activity upon immobilization on surfaces,[12,20] we pattern this protein on Si substrates by μCP-mediated physisorption[22,24] without chemical treatments of involved surfaces.[20] Following the procedure schematized in **Figure 1**, substrates are then incubated in a silica precursor (tetraethylorthosilicate, TEOS) solution and the formation of biosilica is monitored over time. Patterns of recombinant silicatein present well-defined microstructures as evidenced by fluorescence microscopy (**Figure 2**a,b, which correspond to the schematics in the bottom insets of Figure 1a). Physisorption typically relies on interactions between the surface and amino-acidic side-groups of proteins as ruled by hydrophobic, dipolar, electrostatic weak forces. Being the amino-acidic side groups distributed across the entire protein surface, the number of binding points is very large and the layer of biomolecules resulting from exposing the protein solution to a surface is often irreversible and relatively stable. Our pattern is regularly and faithfully transferred and proteins are homogeneously deposited within the stripes. No appreciable fluorescence signal is detected between neighbor printed features, suggesting that the proteins do not significantly diffuse in the channels of the used elastomeric elements. Scanning electron microscopy (SEM) highlights that upon biomineralization the pattern is still clearly visible, thus indicating the onset of silica formation at the printed proteins regions (Figure 2c,d). In other words, the early-stage mineralization process pertains only to areas where silicatein is present, and the neo-formed inorganic material is distributed uniformly along the pre-patterned protein features. Fluorescence microscopy[25] confirms that after 12-24 hs of precursor incubation the silica formation is mainly limited to the protein regions, with Si stripes clearly appreciable between patterned features (**Figure 3**a). Increasing the incubation time, the area covered by biosilica increases as well (as in the scheme in the bottom insets of Figure 1b), extending almost completely over the substrate, with adjacent features tending to merge after 48-72 hs (Figure 3b,c). Finally, for $t_{inc} \geq$ 120 hs, the silica layer results in an almost continuous film (Figure 3d, corresponding to the scheme in Figure 1c). In the absence of precursors, no pattern is observable (negative control of the used staining method), whereas a green fluorescence signal from the silica-staining dye is clearly notable along the stripes after 24 hs of incubation, then progressively extending over the surface upon increasing t_{inc}. This mechanism is in agreement with natural biosilica formation in sponges, whose siliceous spicules exhibit silica growth beginning around the axial filament (mainly made of silicatein), then forming concentric layers with thickness from about 0.3 to 1 μm.[14] We envisage for the formation of our layers a similar process, with a printed protein core promoting silica precipitation and a decrease in organic content upon moving to the periphery of the realized structures.[15b] Also in *Suberites domuncula* and other demosponge species, spicules comprise silicateins mainly in the core filament, suggesting the capability to promote the growth of silica at a distance of a few μm from the biomineralization onset sites along the axis.

We believe that sub-micrometer-sized primary particles gradually aggregate to form larger silica microparticles.[26] In a recent study, nanospheres with a diameter as low as 2.8 nm are reported as basic units of silica in the siliceous spicules,[27]

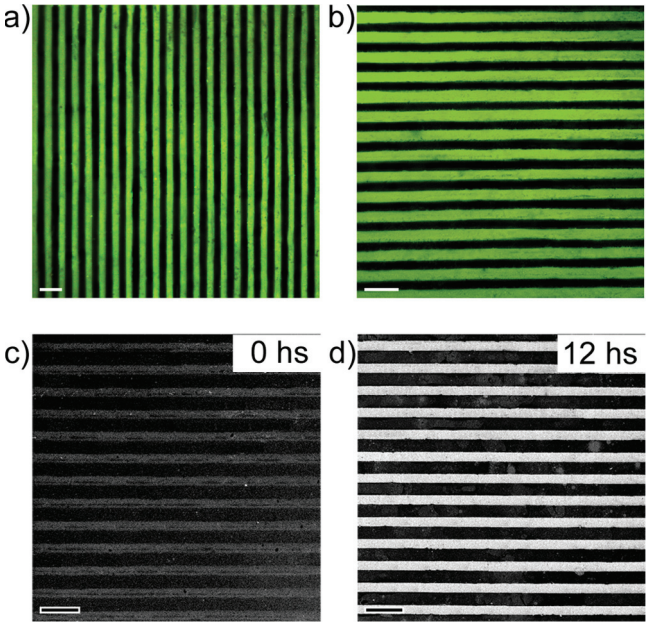

Figure 2. (a,b) Fluorescence microscopy images of FITC-labeled silicatein patterns. Bar: 50 μm. (c, d) SEM images of patterned silicatein (c) and of grown biosilica (d) after precursor incubation. The dark stripes are Si background regions, the brighter stripes are instead regions of patterned silicatein (c) or biosilica (d), respectively. Bar: 50 μm.

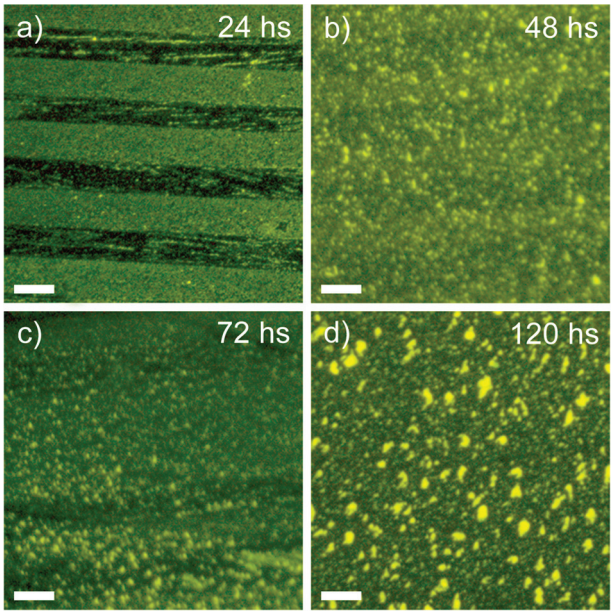

Figure 3. Fluorescence microscopy images of growing silica structures after dye staining. Bar: 50 µm.

whereas here observed stained particles exhibit diameter up to microscale. This difference can be attributed to the gradual aggregation to larger silica microparticles[26] and to different incubation conditions, such as the higher silica concentration with respect to the ambient silica concentration present in the seawater where the animals live.[28] Atomic force microscopy (AFM) confirms that, during our process, the pattern period in the biomineralized layer is almost constant around 85 µm, as determined by the original master template, whereas the biosilica duty cycle (width of silica feature/pattern period) increases from about 0.5 for as-patterned silicatein to 1.0 (i.e., to 100% biosilica coverage of the surface), with a lateral growth-rate of about 300 nm h^{-1} (**Figure 4**a). Overall, we infer that for long t_{inc} the produced biosilica fills effectively empty spaces between adjacent printed protein features, thus giving rise to extended biosilica layers. Instead, control experiments applying this method to non-enzymatically working proteins such as BSA evidence ineffective biomineralization. After TEOS incubation, BSA patterns are unaltered, but no silica formation occurs (Figure S1 in the Supporting Information). Upon silica staining, no mineralized residues are collected after washing even for long t_{inc} (120 hs), which demonstrates that patterning an ordinary protein is not sufficient for realizing silica layers, the use of a biomineralizing protein, i.e. the silicatein, being instead crucial. A significant slower condensation of TEOS[10] and weaker hydrolytic activity (Figure S2 in the Supporting Information) is found for such barely templating proteins with respect to silicatein.

While µCP[29] and transfer molding[30] have been used to pattern surface-passivating agents for the subsequent, selective adsorption of tertiary amine-containing polymer or poly-L-lysines directing biomineralization, the potential use of the resulting features as electrically-insulating films has never been explored. To investigate this issue in depth, conductivity measurements are carried out on native silicatein films and on biomineralized layers after incubation in precursor solution for different time intervals. By applying voltages in the range 0–10 V to a two-terminal configuration, both (i) silicatein microstructures (i.e. before incubation, see the curve at zero incubation time in Figure S3) and (ii) substrates incubated in bare precursor solutions (i.e. without underlying enzyme microstructures) carry currents up to few mA (Figure S3). Therefore, one concludes that (i) printed silicatein does not have electrically-insulating properties per se, i.e. it does not block current, and that (ii) a similar consideration also holds for possible precipitates not mediated by silicatein. Hence, the bare protein microstructure fails in blocking current. On the contrary, biosilica layers formed after 120-132 hs of incubation (with thickness estimated of 200 and 220 nm, respectively) exhibit currents down to the nA range (Figure 4b), corresponding to leakage current densities around 10^{-5} A cm^{-2} through the dielectrics. We point out that our experimental configuration, not using a surface uniformly covered with proteins, allows to probe the insulating properties

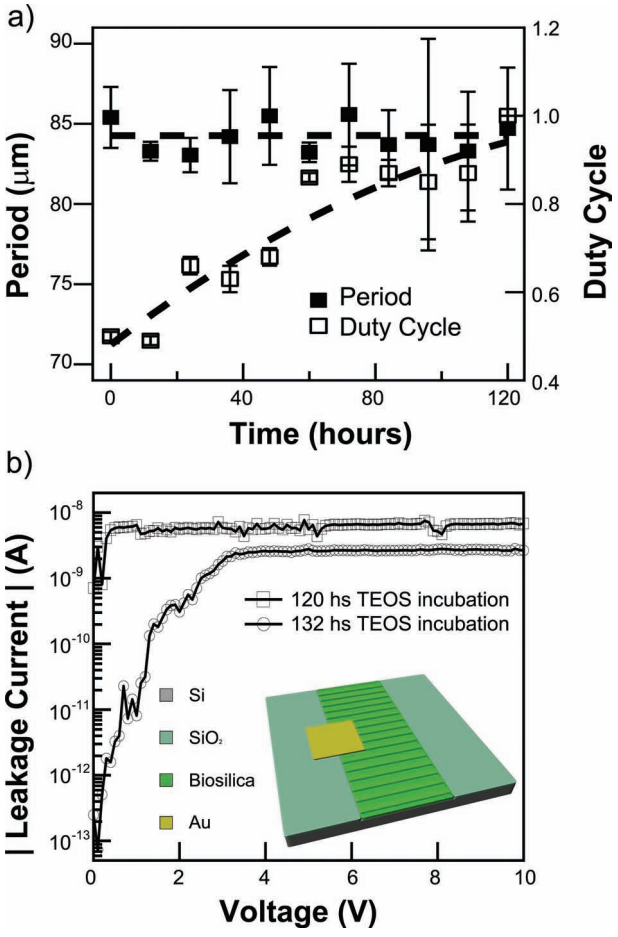

Figure 4. (a) Silica pattern period (full squares) and duty cycle (open squares) vs precursor incubation time. Dashed lines are guides for the eye. (b) 2-contact measurements of leakage current through biosilica layer after 120 (squares) and 132 (circles) hs of TEOS incubation. A scheme of sample preparation for electrical characterization is shown as inset (features not in scale).

of bare biosilica formed in the regions between neighbor silicatein features (scheme in Figure 1c). Also the enhancement of the insulating properties of the biosilica upon increasing t_{inc} can be explained by the formation and aggregation of silica particles,[31] which likely progressively fills defects and local inhomogeneities of the dielectric layer.

In summary, these results extend biosilicification to the controlled fabrication of silica layers with electrically-insulating properties by physiological processing. Patterning recombinant silicatein to realize silica dielectrics can be particularly useful for producing electrical insulating elements in microelectronics[8] under mild conditions, and bioactive materials for biomedical applications.[2,32]

Experimental Section

Materials: Chemicals are obtained from Sigma Aldrich (St Louis, MO), unless otherwise specified. Si slices with a 400 nm-thick SiO_2 layer and *n*-type (As doped) silicon (100) wafers with low resistivity (< 6 mΩ • cm) are purchased from Si-Mat (Kaufering, Germany) and carefully cleaned in a piranha solution of H_2SO_4: H_2O_2 in volume ratio 5:1 at 120 °C for 15 minutes prior use. Photoresists (Nano™ SU8 2025 and 2050) are by MicroChem Corp. (Newton, MA). Poly(dimethylsiloxane) (PDMS) Sylgard 184 by Dow Corning Corp. (Midland, MI) is used with a *A*:*B* (base:curing agent) ratio of 9:1.

Recombinant silicatein production: As reported,[13,14b] the silicatein-α cDNA from *S. domuncula* is inserted into the oligohistidine expression vector pQ30 (Qiagen, Hilden, Germany). The *E. coli* host strain Novagen BL 21 (Merck, Darmstadt, Germany) is transformed with this plasmid and harvested in a BIOSTAT Aplus bioreactor (Sartorius Stedim Biotech, Aubagne, France). The expression of the fusion protein is induced by addition of isopropyl β-D-thiogalaktopyranosid. After collection, the insoluble protein is purified by affinity chromatography and refolded. An optical test, based on the release of aminomethyl coumarin (AMC) from carbobenzoxy-L-phenylalanyl-L-arginyl-4-methylcoumaryl-7-amide Z-Phe-Arg-MCA, is used for testing the hydrolytic activity of the recombinant silicatein compared to other proteins (Supporting Information).

Master production and μCP: Si/SU8 master structures are microfabricated by optical lithography on SU8 [UV-exposure for 20 s at 350 W with an EVG620 mask aligner (EVGroup, St. Florian am Inn, Austria)]. The so obtained features are parallel stripes of period of about 30 and 80 μm (duty cycle ≅ 50%), with height of 15 and 40 μm, respectively. PDMS negative copies of the masters are obtained by replica molding through *in situ* polymerization at 75 °C for 20 minutes. After peeling off, molds are temporarily activated by a 50 W oxygen plasma for 5 s (Tucano, Gambetti Kenologia, Milan, Italy). Then, the elastomeric stamps are immediately inked with the recombinant silicatein solution (50 μg/mL) and left in incubation at 4 °C over 2 hs, allowing biomolecules to physically adsorb onto the PDMS patterned surface. Control experiments are performed by BSA in Phosphate Buffered Saline (pH 7.4, protein concentration of 50 μg/mL). The stamps are then dried by removing the excess solution, left under laminar air flow for few minutes, and put in contact for 2 hs with the Si substrate surface. After gently peeling-off the replicas, patterned substrates are washed with MilliQ water and dried with nitrogen.

Pattern characterization: Fluorescein isothiocyanate (FITC) in dimethyl sulfoxide (DMSO) is used for fluorescence staining of protein patterns[33]. Bicarbonate buffer ($NaHCO_3$ solution A; 3.5 mL, 0.1 M) is mixed with carbonate buffer (Na_2CO_3 solution B; 315 μL, 0.1 M). Substrates are incubated in A + B (1.3 mL) with addition of FITC/DMSO solution (100 μL, 1.5 mg/mL), at 4°C for 8 hs under shaking conditions. Afterwards, they are washed 3 times with PBS (5 minutes each) and immediately observed by a Leica MZ16FA stereomicroscope (Leica Microsystems, Wetzlar, Germany).

Biomineralisation: Patterns (period ≅ 80 μm) and substrates without protein (as negative control) are incubated in TEOS (purity ≥99.0%) at room temperature, up to 120 hs (Figure 1). At different time points, samples are washed with ethanol to remove unreacted TEOS and the biosilica formation is assayed by SEM, AFM, and rhodamine 123 (R123) staining. SEM is carried out by a 150 Turnkey system (Raith, Dortmund, Germany), with acceleration voltage of 5 kV and no prior metal deposition to avoid morphological variations and damages on samples. A Nanoscope IIIa Multimode AFM (Veeco, Plainview, NY) is employed in tapping mode, equipped with different scanners (maximum scan size in the range 15-120 μm), to quantify the lateral and vertical biosilica growth. Phosphorus (*n*) doped Si probes (Veeco) are employed with a resonant frequency of about 270 kHz, and tip radius below 10 nm. R123 is used for staining biosilica,[25] incubating substrates in a R123/phosphate buffer solution (PBS; 1 μg/mL) for 24 hs. Samples are washed three times by PBS, and inspected by a stereomicroscope. For negative controls on BSA samples, R123 and FITC staining are carried out after the biomineralization step.

Electrical characterization: Si substrates are used after completely removing pristine SiO_2 oxide on the surface by photolithography and HF etching, thus exposing 1 mm-wide and 1 cm-long Si windows. For μCP, PDMS replicas are aligned with their parallel features perpendicular to the long side of the Si window. After biomineralization, two-contacts electrical measurements are performed on the silica films in a metal-insulator-metal (MIM) configuration, using a highly *n*-type doped Si substrate and a 100-nm thick Au electrode as bottom and top electrodes, respectively. Au is deposited by Physical Vapour Deposition (PVD75, Kurt J. Lesker, Clairton, PA) on top of the silica film at 1 Å/s and pressure of 10^{-6} mbar. This procedure allows to define a 100 μm × 100 μm region across the Si/biosilica edge, partially covering silica and hence suitable for electrical measurements. The characterization system includes two manual miniature probeheads (PH100, Süss Micro Tec AG, Garching, Germany), a semiconductor parameter analyzer (4200 SCS, Keithley Instruments Inc. Cleveland, OH) and a stereomicroscope (SZ61-TR, Olympus, Milan, Italy) for device inspection and careful probe positioning without damaging the biosilica layers. Each micrometric probehead is connected to a W probe tip (tip radius below 1 μm) for accurate contacting. The electrical continuity across Au is assessed as well before measurements.

Supporting Information

Supporting Information is available from the Wiley Online Library or from the author.

Acknowledgements

This work is financially supported by the BIO-LITHO European project (6th Framework Program, NMP). W.E.G. Müller is holder of an ERC Advanced Research Grant.

Received: July 14, 2011
Published online: September 12, 2011

[1] T. Lebold, C. Jung, J. Michealis, C. Bräuchle, *Nano Lett.* **2009**, *9*, 2877.
[2] M. Wiens, X. Wang, H. C. Schröder, U. Kolb, U. Schloßmacher, H. Ushijima, W. E. G. Müller, *Biomaterials* **2010**, *31*, 7716.
[3] A. J. Mieszawska, L. D. Nadkarni, C. C. Perry, D. L. Kaplan, *Chem. Mater.* **2010**, *22*, 5780.
[4] H. C. Schröder, O. Boreiko, A. Krasko, A. Reiber, H. Schwertner, W. E. G. Müller, *J. Biomed. Mater. Res B* **2005**, *75*, 387.
[5] M. Cerruti, N. Sahai, *Rev. Mineral. Geochem.* **2006**, *64*, 283.

[6] L. L. Hench, J. Wilson, *Science* **1984**, *226*, 630.
[7] B. Bhushan, *Handbook of Nanotechnology*, New York, Springer, **2010**.
[8] a) R. A. Street, *Adv. Mater* **2009**, *21*, 2007; b) G. Gelinck, P. Heremans, K. Nomoto, T. D. Anthopoulos, *Adv. Mater*. **2010**, *22*, 3778.
[9] R. K. Iler, *The Chemistry of Silica: Solubility, Polymerization, Colloid and Surface Properties, and Biochemistry*, New York, Wiley, **1979**.
[10] J. N. Cha, K. Shimizu, Y. Zhou, S. C. Christiansen, B. F. Chmelka, G. D. Stucky, D. E. Morse, *Proc. Natl. Acad. Sci. USA* **1999**, *96*, 361.
[11] H. C. Schröder, X. Wang, W. Tremel, H. Ushijima, W. E. G. Müller, *Nat. Prod. Rep*. **2008**, *25*, 455.
[12] X. Wang, M. Wiens, H. C. Schröder, S. Hu, E. Mugnaioli, U. Kolb, W. Tremel, D. Pisignano, W. E. G. Müller, *Adv. Eng. Mater.* **2010**, *12*, B422.
[13] U. Schloßmacher, M. Wiens, H. C. Schröder, X. Wang, K. P. Jochum, W. E. G. Müller, *FEBS J.* **2011**, doi: 10.1111/j.1742-4658.2011.08040.x.
[14] a) J. C. Weaver, D. E. Morse, *Microsc. Res. Techniq*. **2003**, *62*, 356. b) S. E. Wolf, U. Schloßmacher, A. Pietuch, B. Mathiasch, H. C. Schröder, W. E. G. Müller, W. Tremel, *Dalton Trans.* **2010**, *39*, 9245.
[15] a) R. Cattaneo-Vietti, G. Bavestrello, C. Cerrano, M. Sarà, U. Benatti, M. Giovine, E. Gaino, *Nature* **1996**, *383*, 397; b) J. Aizenberg, V. V. Sundar, A. D. Yablon, J. C. Weaver, G. Chen, *Proc. Natl. Acad. Sci. USA* **2004**, *101*, 3358.
[16] A. Krasko, B. Lorenz, R. Batel, H. C. Schröder, I. I. M. Müller, W. E. G. Müller. *Eur. J. Biochem*. **2000**, *267*, 4878.
[17] a) S. D. Pogula, S. V. Patwardhan, C. C. Perry, J. W. Gillespie, S. Yarlagadda, K. L. Kiick, *Langmuir* **2007**, *23*, 6677; b) M. Xu, G. M. Gratson, E. B. Duoss, R. F. Shepherd, J. A. Lewis, *Soft Matter* **2006**, *2*, 205; c) L. L. Brott, R. R. Naik, D. J. Pikas, S. M. Kirkpatrick, D. W. Tomlin, P. W. Whitlock, S. J. Clarson, M. O. Stone, *Nature* **2001**, *413*, 291; d) E. A. Coffman, A. V. Melechko, D. P. Allison, M. L. Simpson, M. J. Doktycz, *Langmuir* **2004**, *20*, 8431; e) D. J. Kim, K.-B. Lee, Y. S. Chi, W.-J. Kim, H. Paik, I. S. Choi, *Langmuir* **2004**, *20*, 7904.
[18] H. R. Luckarift, S. Balasubramanian, S. Paliwal, G. R. Johnson, A. L. Simonian, *Colloids Surf. B* **2007**, *58*, 28.
[19] A. Rai, C. C. Perry, *Silicon* **2009**, *1*, 91.
[20] M. N. Tahir, P. Théato, W. E. G. Müller, H. C. Schröder, A. Janshoff, J. Zhang, J. Huthe, W. Tremel, *Chem. Commun.* **2004**, 2848.
[21] A. Rai, C. C. Perry, *Langmuir* **2010**, *26*, 4152.
[22] Y. Xia, G. M. Whitesides, *Angew. Chem. Int. Ed.* **1998**, *37*, 550.
[23] S. A. Ruiz, C. S. Chen, *Soft Matter* **2007**, *3*, 1.
[24] N. Sgarbi, D. Pisignano, F. Di Benedetto, G. Gigli, R. Cingolani, R. Rinaldi, *Biomaterials* **2004**, *25*, 1349.
[25] W. E. G. Müller, M. Rothenberger, A. Boreiko, W. Tremel, A. Reiber, H. C. Schröder, *Cell Tissue Res.* **2005**, *321*, 285.
[26] T. Coradin, P. J. Lopez, *ChemBioChem* **2003**, *4*, 251.
[27] A. Woesz, J. C. Weaver, M. Kazanci, Y. Dauphin, J. Aizenberg, D. E. Morse, P. Fratzl, *J. Mater. Res.* **2006**, *21*, 2068.
[28] H. C. Schröder, F. Natalio, I. Shukoor, W. Tremel, U. Schloßmacher, X. Wang, W. E. G. Müller, *J. Struct. Biol.* **2007**, *159*, 325.
[29] D. J. Kim, K.-B. Lee, T. G. Lee, H. K. Shon, W-.J. Kim, H. Paik, I. S. Choi, *Small* **2005**, *1*, 992.
[30] R. Butler, N. Ferrell, D. Hansford, R. Naik, *J. Mater. Res.* **2009**, *24*, 1632.
[31] C. C. Perry, *Rev. Mineral. Geochem.* **2003**, *54*, 291.
[32] F. Natalio, T. Link, W. E. G. Müller, H. C. Schröder, F.-Z. Cui, X. Wang, M. Wiens, *Acta Biomater.* **2010**, *6*, 3720
[33] A. B. Schreiber, J. Haimovich, *Methods Enzymol.* **1983**, *93*, 147.